J. Phycol. **51,** 1055–1065 (2015)

DOI: 10.1111/jpy.12345

SEASONAL SUCCESSION OF THE TRAVERTINE-FORMING DESMID *OOCARDIUM STRATUM*[1]

Caroline Linhart

Department of Medical Statistics, Informatics, and Health Economics, Medical University Innsbruck, Schöpfstraße 41/1, Innsbruck 6020, Austria

and Michael Schagerl[2]

Department of Limnology and Oceanography, University of Vienna, Althanstrasse 14, Vienna A-1090, Austria

The calcifying Conjugatophyte *Oocardium stratum* occurs exclusively in spring-associated limestones (SAL) with active meteogene limestone deposition. The macroscopic colonies of *Oocardium stratum* form hemispherical, pinhead-like structures with a diameter of 0.5–2.0 mm. As its autecology is still poorly understood, we focused on the seasonal development of *Oocardium stratum* and linked environmental factors to its abundance. The study was conducted in a rivulet in Lunz/See (Austria) for 16 months on a weekly (growing season) to monthly (winter season) basis. *Oocardium* colonies were found throughout the whole year, with maximum abundance during the mid-summer months July and August. Repeated macro-mapping of three SAL sites measuring 750 cm^2 each showed a maximum *Oocardium* cover of around 30% in August; two smaller peaks developed in early summer and late autumn with ~10% cover. Diatom mats dominated by *Cymbella excisiformis* occurred in spring, autumn and winter, with more than 75% cover. The seasonal change between *Oocardium* and diatoms in limestone-precipitating springs causes a typical sequence pattern of limestone layers. Redundancy analysis revealed water temperature and bicarbonate content as the main structuring factors; these control the occurrence and growth of *Oocardium*, reflecting season as a background variable. Optimum growth conditions for *Oocardium* were an alkalinity around 4.7 meq $\cdot L^{-1}$ and a water temperature around 13°C. Site openness, nitrate and dissolved carbon dioxide were inversely related to *Oocardium* biomass, the opposite for diatoms. Other environmental factors such as total ions or soluble reactive phosphorus had no significant influence on *Oocardium stratum* abundance.

Key index words: **alkalinity; calcification; diatom; SAL; spring; travertine; tufa**

***Abbreviations*: DCA, detrended correspondence analysis; N-NH_4, ammonium-N; N-NO_2, nitrite-N; N-NO_3, nitrate-N; PCA, principal component analysis; RDA, redundancy analysis; SAL, spring-associated limestones; SRP, soluble reactive P; WA, weighted average**

The desmid *Oocardium stratum* Nägeli is restricted to active meteogene travertine springs (Pentecost 2005) and headstreams, which was recently termed spring-associated limestones (SAL) by Sanders et al. (2011). *Oocardium stratum* grows on various surfaces encrusted with carbonate. Active and intact SAL habitats without anthropogenic pollution are rare (Sanders et al. 2011, Cantonati et al. 2012b), but exist in limestone areas all over the world. The macroscopic colony-structure of the greenish *O. stratum* resembles green pinheads. The *Cosmarium*-like cells (width 15–20 μm, length 10–20 μm) are located at tips of gelatinous stalks encrusted with lime (Wallner 1933, 1934a,b, Golubić and Marčenko 1958, Schagerl and Pröschold 2007). *Oocardium stratum* has been documented for North America (Mathews et al. 1965, Pfiester 1976), Cuba, India (Rieth 1969), China (Pentecost and Zhang 2000) and a few locations all over Europe (e.g., Nägeli 1849, Wallner 1934c, Rieth 1969, Pfiester 1976, Coesel 2002, Rott et al. 2012, Moreno Alcaraz et al. 2013). For eastern Austria, *O. stratum* was documented by Hansgirg (1905) near Wiener Neustadt and by Brehm and Ruttner (1926) in the area of Lunz/See. Later on, it seemed to have disappeared; Lenzenweger (2003) did not include this taxon in the flora of Austrian desmids. Schagerl and Pröschold (2007) rediscovered *O. stratum* in a small rivulet at the Mayrgraben in Lunz/See. Subsequently, Sanders and Rott (2009) studied two more sites in western Austria; Rott et al. (2012) described a third location in Tyrol. Because of its special habitat, it is easily overlooked and probably more frequent than reported (Pfiester 1976).

The characteristics of SAL are reviewed in detail by Pentecost (2005) and Sanders et al. (2011), the latter work providing detailed information of SAL

[1]Received 1 March 2015. Accepted 16 August 2015.
[2]Author for correspondence: e-mail michael.schagerl@univie.ac.at.
Editorial Responsibility: M. Posewitz (Associate Editor)

formation in the Eastern Alps. Basically, groundwater enriched in dissolved carbon dioxide dissolves carbonates, forming a solution of calcium bicarbonate. Upon reaching the surface, carbon dioxide becomes supersaturated, degasses into the atmosphere and causes carbonates to precipitate on any available surface. Pentecost (2005) classified travertine based on their carrier carbon dioxide, which may originate from soil by respiration activities (meteogene) or from processes in deeper earth layers where higher temperature is an additional factor for dissolving carbonates (thermogene). *O. stratum* is mentioned to have a patchy distribution because of its restricted occurrence solely in SAL habitats (Pentecost 2005).

To date, only scarce information is available on the autecology of *O. stratum* (Wallner 1933, 1934a,b, Pentecost 1981, 1991, 1993, 2005, Sanders and Rott 2009). Rott et al. (2010) observed that *O. stratum* colonies are found only at a certain distance from the spring and their occurrence extends over 2/3 of the full length of the limestone-precipitating stretch, which indicates a very peculiar spatial niche even within the SAL headstream. Recent studies focusing on SAL formation and lamination induced by *O. stratum* have been conducted by Sanders and Rott (2009), who suggested that seasonal changes in irradiance control the presence/absence of *O. stratum* and therefore the seasonal layering of carbonate. Limestone deposition showed a high increase up to 5 mm $\cdot$ a^{-1} during warmer periods induced by intense *Oocardium stratum* growth, and a strong reduction caused by massive development of benthic diatoms in autumn and winter. Rott et al. (2010) focused on the community composition in two SAL systems and also considered the morphology of *Oocardium*. The NO_3-N concentration between both sites differed by a factor of 10 (10.5 mg $\cdot$ L^{-1} at Lingenau, ~1 mg $\cdot$ L^{-1} at Alpenzoo); total phosphorus amounts were mentioned to be low, but no data were provided. A few other studies on this taxon focused mainly on SAL formation; the ecological niche of *Oocardium* was largely neglected.

So far, seasonal biomass fluctuations of *O. stratum* and studies to define key variables of temporal patterns have not been conducted. We therefore designed a cross-seasonal case study to shed light on the habitat characteristics and seasonal succession of *O. stratum*. We also included winter-sampling to study occurrence of *Oocardium* during snow cover of the rivulet. Most of the studies conducted so far included low sampling frequencies; we sampled the location in short time intervals over a period of 16 months to get detailed insight into the development of the *Oocardium* community. We applied digital macro-mapping to reveal *O. stratum* cover over time, which was finally linked to environmental conditions.

MATERIAL AND METHODS

Study site. The small SAL headstream "*Oocardium* rivulet" is part of the southwest-faced slope Mayrgraben system in Lunz am See (47°15 N, 15°04 E) located in the limestone alps of Lower Austria at 714 m above sea level (Fig. 1). The geological catchment area of the spring system is part of the Lunzer beds II (Sulzbach beds) next to the Ötscher nappe (Tollmann 1965) and belongs to the geological era of Upper Eastern Alps Mesozoic (Faupl 2003). This nappe system includes mainly karst formations such as Gutensteiner limestone, Werfener banks and dolomite (Götzinger 1910, Leichtfried 1990). Both the *Oocardium* rivulet (= SAL rivulet) and the Mayrbach rivulet are located in a sandstone and shale formation of the Lunzer beds (Fig. 2). The riparian vegetation comprises mainly *Fraxinus excelsior* Linné, *Picea abies* Karst, *Fagus sylvatica* Linné, and *Rubus* subgen. *rubus* Linné. Mean annual precipitation in Lunz am See is ~1,740 mm $\cdot$ a^{-1} and the mean annual air temperature is 7.4°C (ZAMG 2000-2013). We chose four sampling sites in the *Oocardium* rivulet (Fig. 3, A–D) and one more in the main Mayrbach rivulet (E) without active limestone deposition (reference site). Site A is located nearest to the spring, and free of *Oocardium*. The site is characterized by a high amount of incoming irradiance and, here, limestone depositions start to develop. B and C are located in the middle stretch of the headstream; B has natural shading and on site C artificial leaf shading was installed. D is located a few meters upstream of the mouth of the headstream, where it discharges into the Mayrbach rivulet. It is also characterized by high incoming irradiance; both B and D are small SAL cascades. E was chosen as a reference without *Oocardium;* it is located in the Mayrbach rivulet just a few meters upstream of the merging of the *Oocardium* rivulet. *Oocardium* occurs at sites B, C, and D, but not on A and E (Fig. 3).

Data collection. Sampling took place between March 2008 and July 2009. From March to November 2008 we sampled in weekly intervals, in the following winter season until March 2009 on a monthly basis, and from April to July 2009 again in weekly intervals. At each site, data loggers (HOBO UA-002-64 Pendant Data Logger) recorded water temperature (°C) and illuminance (lux) as a proxy for light intensity every two min. For data analyses, the weekly average, daily minimum and maximum of temperature, and weekly sum of incoming irradiance were considered. On site, specific conductivity ($\mu S \cdot cm^{-1}$), water temperature (°C), and oxygen concentration (% and mg $\cdot$ L^{-1}) were measured using a portable multi-Meter (HQ 40d, 10105; Hach Lange, Düsseldorf, Germany). Water discharge ($L \cdot s^{-1}$) was estimated at a point where the streambed narrowed using a bucket and a stopwatch.

Sky openness was calculated by means of hemispherical photos taken with the digital camera Nikon Coolpix 4500 equipped with a Nikon fisheye converter FC-E8 0.21x. The camera was placed on a thin, levelled, and polystyrol plate directly in the headstream. The magnetic north was marked on the lens of the fisheye converter. The photos were post-processed using Adobe Photoshop Version 8.0.1 to eliminate any shading caused by the photographer. The light parameters were then calculated by the computer program Gap Light Analyzer (GLA) Version 2.0 (Frazer et al. 1999). Except for spectral fraction, which was set to 0.45 to adjust for the transmitted photosynthetic active radiation, default settings were used (Frazer et al. 1999, Hainz et al. 2009). For GLA, a growing period has to be defined, which was assumed to be 12 months for *Oocardium*.

Oocardium stratum cover was estimated at B, C, and D by macro-mapping of photos (Olympus µ 1030 SW) from always exact the same fragment (30 cm × 25 cm) using a fixed grid.

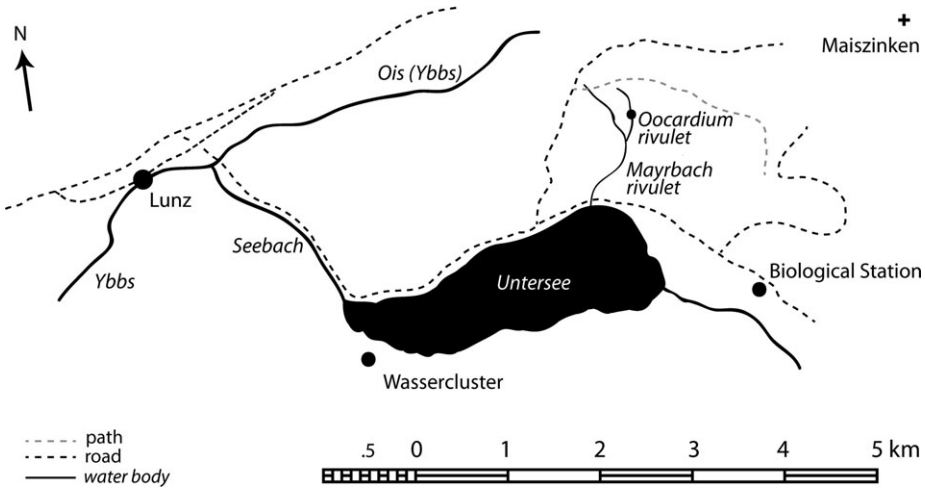

FIG. 1. Location of the sampling sites Oocardium rivulet and Mayrbach rivulet in Lunz/See.

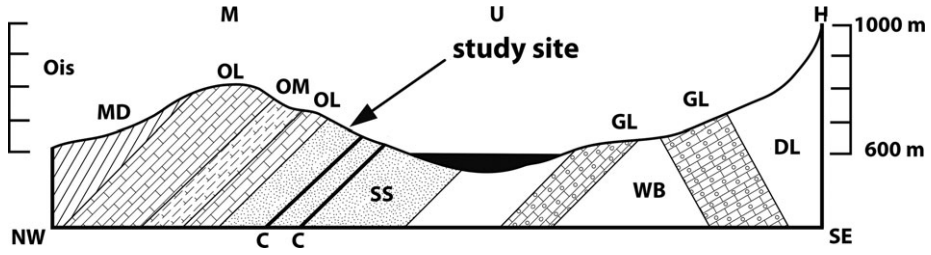

FIG. 2. Geological profile through the lake valley of Lunz from the Maiszinken (M) over the lake Lunzer See (U) to the Hetzkogel (H), Height to length 1:75. MD (Main dolomite), OL (Opponitzer limestone), OM (Opponiter mergel), SS (Sandstone and shale), C (Coal), GL (Gutensteiner limestone), WS (Werfener banks), DL (Dachstein limestone). After Götzinger (1910).

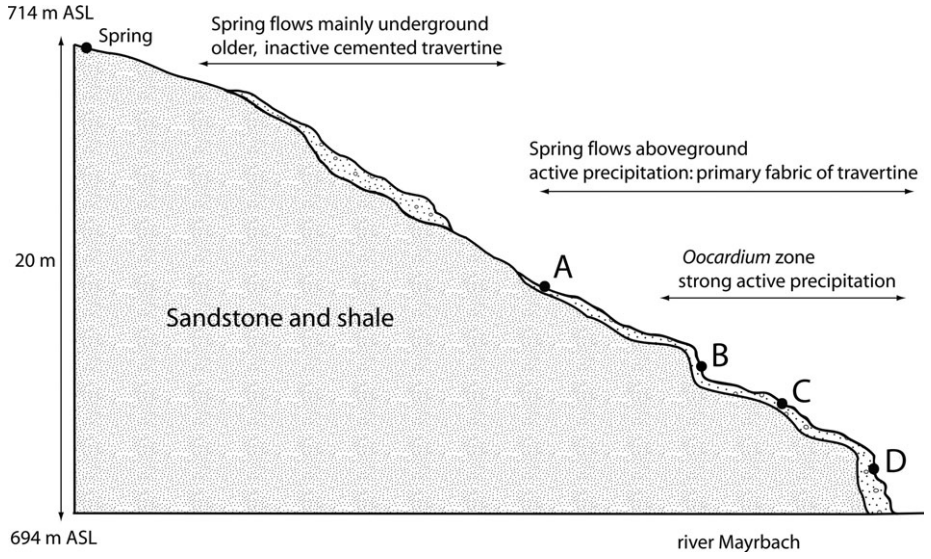

FIG. 3. Altitude profile of study site and positions of sampling sites. The *x*-axis represents the elevation, where the Oocardium Rivulet discharges into the Mayrbach River. The spring of the *Oocardium* River in the Mayrgraben is 714 m above sea level. In the first 40–50 m of the spring, the course of the rivulet is mainly underground. Inactive and cemented travertine indicates the former spring course. At an altitude of 703 m above sea level, the rivulet flows again aboveground and active precipitation starts. Between sites A and B, 65 m downstream of the spring, the *Oocardium* zone starts; it ends an additional 20 m downstream at the confluence with the Mayrbach Rivulet.

Species were identified under a Zeiss Axio Imager.M1 microscope (camera: Axio Cam MRc5, computer application: Axio Vision Release 4.7.2). Following identification keys were used for diatoms: Hofmann et al. (2011), Krammer and Lange-Bertalot (2004-2008). Macro-mapping photos were post-processed with Adobe Photoshop Version 8.0.1 to adjust the same

photographed area and resolution. Three copies of each photo were made: one to quantify all green pixels (*Oocardium*), one to quantify all red pixels (diatoms), and one as a reference picture. The binary pictures of red and green fractions were further analyzed with respect to the amount of overgrown biomass area of *O. stratum*, the moss *Cratoneuron* sp. and diatom mats, respectively, using the computer application ImageJ Version 1.43j (Rasband 1997-2014). The pictures were then converted into 16 Bit greyscale pictures and adjusted to a threshold of 200 to estimate the summarized area of all particles and to calculate the percentage of diatom and *Oocardium* biomass.

For water chemistry, triplicates from each site were taken. We used BOD-bottles to keep the CO_2 pressure in the water samples constant until analysis. Sampling and analyzing was performed according to Legler (1988): bottles were carefully filled with a PVC hose to avoid sparkling and any turbulences with the atmosphere. The bottles were kept cold and dark and were immediately transferred to the laboratory. From filling the water bottles until analyses, no more than 30 min passed. To avoid outgassing of free carbon dioxide during transport, water samples for analysis of carbon species were covered with pentane. Total alkalinity (m value at pH 4.3), pH and acidity (*p* value at pH 8.2) were determined titrimetrically with a Titrino 702 SM (Metrohm Ion Analysis, Switzerland). Soluble reactive phosphorus (SRP), nitrate-N ($N\text{-}NO_3^-$), nitrite-N ($N\text{-}NO_2^-$) and ammonium-N ($N\text{-}NH_4^+$) were analyzed according to the standardized Continuous Flow Method (Eberlein and Kattner 1987, Kempers and Luft 1988, Apha 2012). Magnesium (Mg^{2+}), calcium (Ca^{2+}), sodium (Na^+), chloride (Cl^-), potassium (K^+) and sulphate (SO_4^{2-}) were analyzed by ion chromatography (Metrohm Compact IC 761, Metrohm IC Filtration Sample Processor 788).

Data analyses. Statistical analyses were carried out using the computer program R 2.9.2 GUI 1.29 (R Core Team 2014) including the external software packages nortest, psych, and vegan. All variables were checked for normal distribution using qq-plots and Lilliefors (Kolmogorov–Smirnov) test statistics. If necessary, data transformation was used: $\arcsin\sqrt{x}$ for percentage data like cover and site openness (Dormann and Kühn 2009), sqrt(x) or $\log_{10}(x + 1)$ for other variables (Ramette 2007, Hainz et al. 2009). Since the sample size of 50 limited the number of input variables for the principal component analysis (PCA), a bivariate correlation matrix for all *Ocardium* sites was first calculated including all variables to select adequate input variables for a PCA. Several factors were excluded from the PCA: the sum of ions and HCO_3^- because of high correlation with conductivity, oxygen because of low variation, pH because of high correlation with free CO_2, $N\text{-}NO_2^-$, and $N\text{-}NH_4^+$ because of a very low amount and the better representation of nitrogen supply by $N\text{-}NO_3^-$, and precipitation because discharge has more influence on water chemistry and also considers snowmelt. PCA was performed including all *Oocardium* sites (BCD) into a single model.

To test seasonality of variables involved in the calcium-carbonic acid-equilibrium (free CO_2, HCO_3^-, Ca_2^+ and pH), we used Wilcoxon-test; significant differences between the reference rivulet and the *Oocardium* rivulet were checked with the Mann–Whitney *U*-test.

The synthetic gradient length of biomass data was checked with a detrended correspondence analysis (DCA, decorana within R package vegan) to decide for either unimodal or linear methods. For all tested sites (B, C, D) the gradient length of the first DCA axis was smaller than 2, indicating that the linear ordination method redundancy analysis (RDA) is adequate (Leyer and Wesche 2008, Dormann and Kühn 2009) to gain insight into species-environment relationships. In constrained ordination, two different site scores exist: linear combinations scores (linear combinations of constraining variables) and weighted average (WA) species scores. The vegan package uses WA scores because they are more stable against random error, which is very common in environmental data sets (Oksanen et al. 2007, Oksanen 2011). To extract the best subset of the environmental data set, the function bioenv (package vegan) was used. In this method, the variable selection is based on maximum (rank) correlation of the Euclidean distance of the scaled environmental data with the species dissimilarity matrix (Oksanen et al. 2007). For the final RDA model, we used constraints extracted by permutation tests (at least 999 permutations). A sequential ("Type I") permutation test analyzed the significance of all selected terms separately, and a "Type III" test calculated the marginal effect of each constraining variable, while each variable is removed from the model including all other variables. Also, each axis was tested with a permutation test (Oksanen 2011). In addition, variance inflation factors (VIF) for each variable were checked and variables with a VIF above 10 were excluded to avoid multicollinearity (Oksanen et al. 2007, Dormann and Kühn 2009, Oksanen 2011). In the final model, only significant ($P < 0.05$) and independent variables were used. Sites (B–D) and dates (1–50) were coded and treated as covariables to avoid the problem of pseudoreplication.

RESULTS

Environment. The karst system of the catchment area receives weekly precipitation between 0.2 and 233.2 mm. The discharge of the rivulet was usually between 0.5 and 0.8 $L \cdot s^{-1}$ with two exceptions: during the snowmelt (March 2009) and heavy rainfalls (July 2009), the discharge increased to 6 $L \cdot s^{-1}$ and 3 $L \cdot s^{-1}$, respectively (Table 1). Within the short headstream stretch (distance from spring to mouth 85 m), the annual mean water temperature increased from 8.5°C to 11.3°C. The *Oocardium* rivulet was slightly oversaturated with free CO_2 and O_2 and generally showed very low nutrient concentrations (Tables 1 and 2). The stretch from A to D clearly revealed a drop of free carbon dioxide, conductivity, and also slightly decreasing Ca^{2+} concentrations (Table 1). pH increased downstream; the lowest pH was related to the highest amounts of free carbon dioxide near the spring (site A). The most prominent cation in the *Oocardium* rivulet was Ca^{2+}, with an annual median of 2.03 $mM \cdot L^{-1}$ (81.0 $mg \cdot L^{-1}$), followed by Mg^{2+} with 0.27 $mM \cdot L^{-1}$ (6.5 $mg \cdot L^{-1}$). The dominant anion was HCO_3^- with 4.5 $mM \cdot L^{-1}$ (274.5 $mg \cdot L^{-1}$; Table 1). High water events such as snowmelts in spring or thunderstorms in summer led to a dilution of mainly Mg^{2+} and SO_4^{2-}. Interestingly, $N\text{-}NH_4^+$ concentrations decreased downstream.

Seasonality was reflected in water chemistry: free CO_2 was significantly lower in summer compared to winter for B, C and D ($P < 0.01$, $n = 16$). The Ca^{2+} concentration was lower in summer than in winter for A and B ($P < 0.05$, $n = 16$), C and D showed no significant Ca^{2+} differences between seasons. Winter and summer pH also showed no significant differences. We also compared the amount of outgassing

TABLE 1. Mean values and standard errors of various variables for each site at the *Oocardium* headwater (A–D), its source ($N = 5$) and from Mayrbach Rivulet (E). For units see Table 2.

	Source	A	B	C	D	E
CO_2	19.33 ± 2.73	3.07 ± 0.63	2.31 ± 0.56	1.61 ± 0.69	1.44 ± 0.60	1.1 ± 1.5
HCO_3^-	5.93 ± 0.04	4.54 ± 0.25	4.49 ± 0.25	4.45 ± 0.25	4.42 ± 0.25	4.7 ± 0.3
pH	7.51 ± 0.07	8.2 ± 0.1	8.3 ± 0.1	8.3 ± 0.1	8.3 ± 0.1	8.4 ± 0.2
Conductivity	516.00 ± 2.35	397.8 ± 20.4	392.5 ± 20.1	388.5 ± 20.2	386.8 ± 20.0	408.7 ± 20.3
$N\text{-}NH_4^+$	13.45 ± 11.18	12.54 ± 24.48	8.21 ± 10.43	6.71 ± 5.15	6.17 ± 4.52	10.2 ± 9.2
$N\text{-}NO_2^-$	0.38 ± 0.67	0.85 ± 0.77	0.80 ± 0.43	0.87 ± 0.41	0.86 ± 0.49	2.5 ± 2.1
$N\text{-}NO_3^-$	1,278.94 ± 14.59	906.03 ± 330.89	909.89 ± 341.15	912.30 ± 347.39	907.55 ± 347.22	964.24 ± 166.34
SRP	7.41 ± 0.65	0.99 ± 1.15	0.55 ± 0.67	0.59 ± 0.88	0.50 ± 0.66	12.5 ± 6.0
Na^+	0.88 ± 0.04	0.77 ± 0.12	0.77 ± 0.19	0.75 ± 0.12	0.74 ± 0.11	1.9 ± 0.5
K^+	1.00 ± 0.09	0.74 ± 0.15	0.75 ± 0.16	0.74 ± 0.14	0.76 ± 0.17	1.4 ± 0.3
Ca^{2+}	105.77 ± 1.68	82.86 ± 4.61	81.36 ± 4.34	79.43 ± 5.64	79.33 ± 4.69	82.4 ± 6.5
Cl^-	0.63 ± 0.04	0.49 ± 0.14	0.48 ± 0.17	0.47 ± 0.10	0.48 ± 0.12	1.4 ± 0.4
Mg^+	8.84 ± 0.43	6.30 ± 1.10	6.42 ± 1.07	6.35 ± 1.05	6.37 ± 1.09	8.0 ± 1.1
SO_4^{3-}	3.19 ± 0.12	2.70 ± 0.32	2.72 ± 0.33	2.70 ± 0.31	2.73 ± 0.34	3.0 ± 0.5
Radiation week sum		84,053 ± 48698	77,869 ± 35808	77,869 ± 35808	46,548 ± 42334	

TABLE 2. Summary of environmental variables of the 4 *Oocardium* sites ($n = 50$, except for nutrients $n = 46$ and ions $n = 36$). min (minimum), Q1 (first quartile), median, Q3 (third quartile), max (maximum), temp (temperature).

	Min	Q1	Median	Q3	Max	Unit
Free CO_2	0.0	1.5	2.1	2.7	5.0	$mg \cdot L^{-1}$
HCO_3^-	3.8	4.3	4.5	4.6	5.2	$mM \cdot L^{-1}$
Oxygen	91.1	99.1	100.3	101.3	105.2	%
pH	8.1	8.3	8.3	8.4	8.5	
Conductivity	337.0	380.0	391.0	402.0	453.0	$\mu S \cdot cm^{-1}$
Temp	3.2	9.3	11.6	13.4	20.5	°C
$N\text{-}NH_4^+$	0.0	3.6	5.8	8.9	164.1	$\mu g \cdot L^{-1}$
$N\text{-}NO_2^-$	0.0	0.5	0.8	1.1	4.8	$\mu g \cdot L^{-1}$
$N\text{-}NO_3^-$	302.1	638.8	836.3	1,127.8	1,769.4	$\mu g \cdot L^{-1}$
N_{tot}	307.2	641.3	849.3	1,138.7	1,777.1	$\mu g \cdot L^{-1}$
SRP	0.0	0.0	0.4	1.0	6.1	$\mu g \cdot L^{-1}$
Na^+	0.6	0.7	0.7	0.8	1.7	$mg \cdot L^{-1}$
K^+	0.4	0.6	0.7	0.8	1.3	$mg \cdot L^{-1}$
Ca^{2+}	59.5	77.4	81.0	84.1	92.7	$mg \cdot L^{-1}$
Mg^{2+}	3.8	5.7	6.5	7.1	8.3	$mg \cdot L^{-1}$
Cl^-	0.3	0.4	0.5	0.5	1.3	$mg \cdot L^{-1}$
SO_4^{2-}	2.0	2.5	2.7	2.9	3.4	$mg \cdot L^{-1}$
Discharge	0.1	0.5	0.6	0.8	6.7	$L \cdot s^{-1}$
Precipitation day	0	0	1.25	5.5	64.8	mm
Precipitation week	0.2	7.4	21.55	50	233.2	mm
Site openess	13.9	28.0	22.4	36.3	50.9	%
Temp week mean	1.3	9.0	11.5	13.8	18.2	°C
Temp day mean	1.1	8.7	10.9	14.1	19.9	°C
Temp day max	2.4	12.1	17.4	22.7	40.9	°C
Temp day min	0.1	6.3	9.1	11.2	15.5	°C
Radiation week mean	1.0	7.2	12.2	18.9	40.7	klx
Radiation week sum	3,457.5	35,515.6	61,481.7	96,394.0	204,924.0	klx
Radiation day mean	0.3	5.1	10.8	19.0	43.2	klx
Radiation day sum	225.2	3,457.3	6,619.1	14,010.4	31,119.6	klx

CO_2 (= difference of dissolved CO_2 between site A and D) between winter and summer: values were slightly higher in the latter ($1.73 mg \cdot L^{-1}$ compared with $1.50 mg \cdot L^{-1}$), but the difference was not significant ($P = 0.07$, $n = 21$).

In spite of canopy cover, the irradiance supply at the *Oocardium* rivulet was higher in summer than in winter. In both years, site A displayed the highest irradiance from mid-April to mid-July. Both the minimum ($3.5 Mlx \cdot week^{-1}$ in October 2008) and the maximum ($205 Mlx \cdot week^{-1}$ in April 2009) of the weekly sum of irradiance supply were measured at C (Table 1).

Contrarily to A–D, the reference site E showed neither any active limestone deposition nor *O. stratum* colonies. Compared to the headwater stream, free CO_2 at site E was significantly lower (Mann–Whitney *U*-test, $P < 0.001$, $n = 50$) and the amount of SRP was higher ($P < 0.001$, $n = 50$). PCA revealed three principal components (PCs) with an eigenvalue beyond 1 explaining 71.7% of the total variance in the data set. PC1 had maximum load-

ings on temperature and N-NO_3^-. PC2 had highest loadings on free CO_2 and PC3 on irradiance (Table S1 in the Supporting Information).

Organisms and their relation to the environment. Colonies of *O. stratum* started to develop 65 m downstream of the spring and were observed mainly on cascades down to the confluence into the Mayrbach rivulet—on a stretch of ~20 m (Fig. 3). Besides *O. stratum*, diatoms dominated by *Cymbella excisiformis* Krammer (Fig. 4) and the mosses *Cratoneuron filicinum* (Hedwig) Spruce and *Palustriella commutata* (Hedwig) Ochyra were identified.

Macro-mapping of the sites B, C and D showed comparable seasonal patterns: *O. stratum* was present year round (range 1%–34% coverage; Fig. S1 in the Supporting Information). From December to late May (winter and spring), its cover was reduced to <5% (Figs. 5 and S1). During this time, the few colonies were mainly found in small dimples of rocks. In early summer (June), *O. stratum* growth increased and yielded a first maximum of ~18% cover until diatom mats developed in early July, coinciding with a decrease in *O. stratum*. This brief decline was followed by a summer maximum with around 34% *O. stratum* cover in July and August; diatom mats were almost absent during this period. September and October were characterized by a drop of *O. stratum*, replaced by diatoms finally dominating the biofilm. A brief increase in *O. stratum* (10% cover) occurred in November after breakdown of the diatom mats. Generally, diatoms dominated in early spring, autumn, and winter (peak value 74%; Figs. 5 and S1). Colony development on macro-mapping sites was patchy. After the colonies reached a diameter of ~5 mm, new colonies started to develop in parallel. Mosses also served as

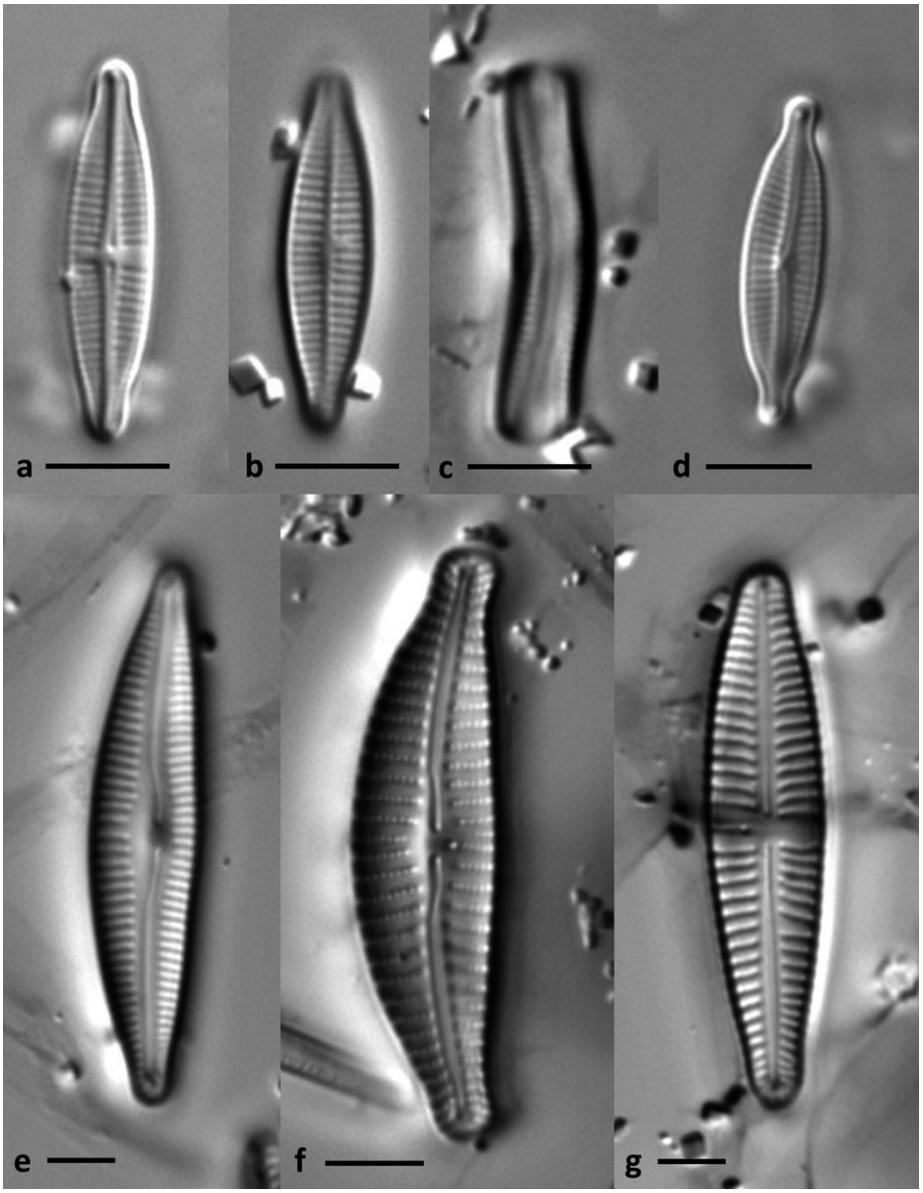

FIG. 4. Diatoms at the *Oocardium* rivulet in Lunz/See (Austria). (a–c) *Achnanthidium minutissimum* (Kützing) Czarnecki, (d) *Encyonopsis microcephala*, (e) *Delicata delicatula*, (f) *Cymbella excisiformis*, (g) *Gomphonema micropus* Kützing, scale bar 5 μm.

substrate for *O. stratum*, especially propagules encrusted with carbonates.

The significant final RDA model (Table S2 in the Supporting Information) considered temperature, HCO_3^-, $N\text{-}NO_3^-$ and site openness and explained 25.3% of total inertia (Table S3 in the Supporting Information). The first RDA axis explained 24.9% of total variance. *Oocardium stratum* occurrence was explained mainly along temperature and HCO_3^- gradients; diatom growth was facilitated by site openness (Fig. 6).

DISCUSSION

Water samples taken directly from the spring were supersaturated with free CO_2, but no active precipitation occurred within the first few meters, most probably due to low gas exchange with the atmosphere. After 5 m, the rivulet disappears for the next 40 m; the riverbed is porous and consists mainly of inactive SAL deposits. In the further course, water emerges again and shows, over the next 40 m, high carbonate precipitation. This process is also reflected in pH and conductivity measurements, with lowest pH and highest conductivity and Ca^{2+} concentration detected at the upstream site A. Downstream, degassing of free carbon dioxide, and carbonate precipitation resulted in a parallel decline of free CO_2, Ca^{2+}, and conductivity. According to the recent definitions and terms of SAL, the rivulet has a moderate size of deposits and a moderate activity status (Sanders et al. 2011).

Studies focusing on biofilms of lotic ecosystems revealed that discharge and stream velocity are key structuring factors for biomass development (Blenkinsopp and Lock 1994, Battin et al. 2003, Besemer et al. 2007). Recent publications, however, indicated that the role of velocity is less important compared to nutrient supply (Passy and Larson 2011). In our survey, the low water discharge frequently observed in summer and autumn coincided with *O. stratum* biomass maxima, but RDA did not reveal a significant contribution of discharge on *O. stratum* occurrence. This is probably because this taxon is resistant against high shear forces through its strong incrustation and calcification (Golubić and

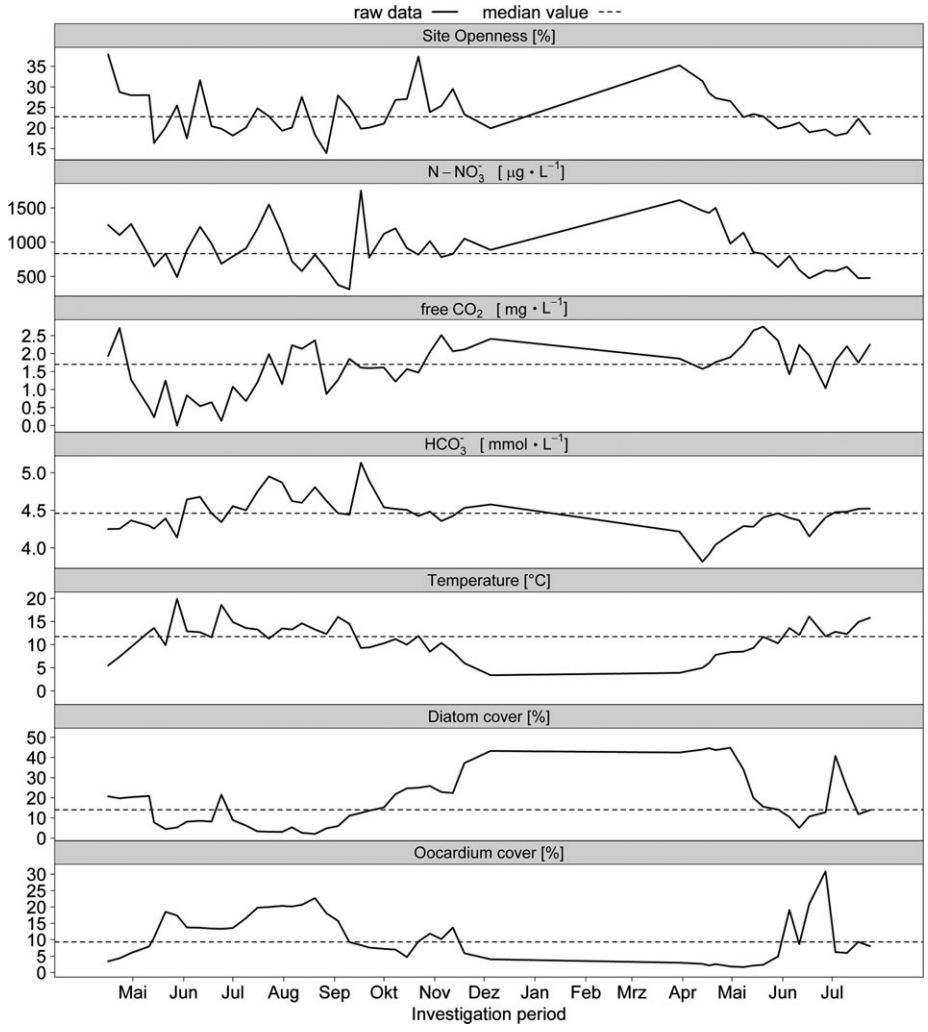

FIG. 5. Seasonal variation in *Oocardium* and diatom cover (macro-mapping) of site C between April 16, 2008 and July 24, 2009 as well as selected environmental variables: temperature (***), bicarbonate (***), free carbon dioxide, nitrate-N and site openness (**). ***$p \leq 0.001$ **$p \leq 0.01$

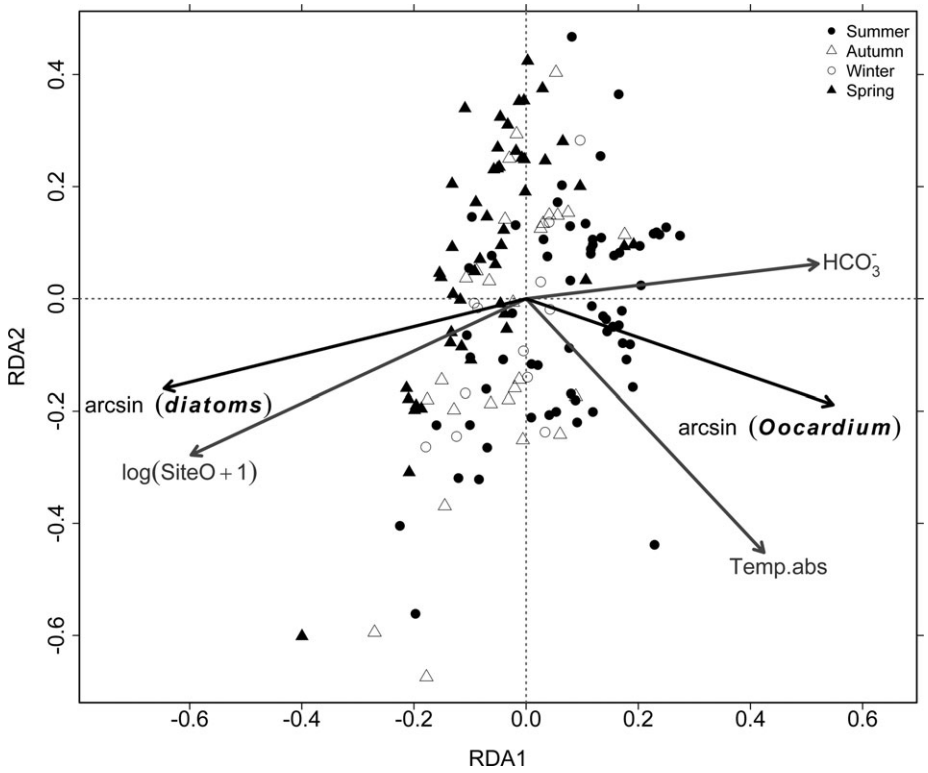

FIG. 6. Redundancy analysis biplot of algal biomass. Presented are the first two axes of the reduced model, with only significant constraints, the transformed variables bicarbonate (HCO_3^-), temperature [°K] (temp.abs), and site openness log (SiteO+1). The sampling sites/times are represented as symbols of seasons for a better representation of the season.

Marčenko 1958). *Oocardium stratum* colonies were eroded only during high water events when even cemented limestone is mobilized (July 2009). *Oocardium stratum* can probably cope with different flow regimes, but direct flow velocity measurements close to the colonies are still lacking. Few data are available on the discharge of *Oocardium* rivers: Sanders and Rott (2009) mentioned a discharge of 1–2 $L \cdot s^{-1}$ for the *Oocardium* site in Lingenau and 5–10 $L \cdot s^{-1}$ for the Alpenzoo site, both located in Austria. Pentecost (1991) referred to two *Oocardium* sites on the British Isles with discharge rates of 0.5–5.0 $L \cdot s^{-1}$ and 40–200 $L \cdot s^{-1}$ and one in Belgium with 10 $L \cdot s^{-1}$.

Water chemistry data on *O. stratum* sites are rare (Pentecost 1991, Sanders and Rott 2009, Rott et al. 2010), but Rott et al. (2012) recently added more detailed information for SAL. Temperature, pH obtained by Pentecost (1991) from the British Isles and Belgium were comparable to our results, as well as and SRP values (0.02–4.60 $\mu M \cdot L^{-1}$ measured by Pentecost and close to detection limit of 0.016 $\mu M \cdot L^{-1}$ in *Oocardium* Rivulet in Lunz/See), but $N\text{-}NH_4^+$ and Ca^{2+} amounts were much higher at our site. Also ion concentrations were slightly higher at our location (Tables 1 and 2). Compared with alpine sites (Sanders and Rott 2009, Rott et al. 2012), the *Oocardium* rivulet in Lunz/See showed only moderate levels of ions including bicarbonate and nutrients (except for $N\text{-}NO_3^-$).

Phosphate levels are generally low in meteogene and thermogene travertine springs due to precipitation of calcium phosphate and its low solubility (Pentecost 2005). The *Oocardium* rivulet showed SRP amounts close to the detection limit (Tables 1 and 2), and total phosphorus levels between 10 and 23 $\mu g \cdot L^{-1}$ (0.32 and 0.74 $\mu M \cdot L^{-1}$) in late spring and summer, respectively, have been obtained in another study (unpublished data). *Oocardium* sites in western Austria also indicated low phosphate levels (Sanders and Rott 2009, Rott et al. 2010). Rott et al. (2012) mentioned ultraoligotrophic conditions for five *Oocardium* sites in the Eastern Alps. Compared to middle and lower courses (Whitton and Neal 2011), SAL habitats show considerably lower P amounts. As P limitation cannot be ruled out, the effect of phosphate availability on the algae community in these habitats needs further attention. Although Bothwell (1989) found saturation of cellular P already at concentrations at around 1 $\mu g \cdot L^{-1}$ (0.03 $\mu M \cdot L^{-1}$) for very thin diatom biofilms, maximum periphyton biomass still showed responses to increasing P supply until P levels of around 30 $\mu g \cdot L^{-1}$ (0.97 $\mu M \cdot L^{-1}$). Many benthic algae in streams show surface phosphatase activity (Whitton et al. 2005), which indicates P limitation. In this concern, the highly interesting taxon *Didymosphenia geminata* (Lyngbye) Schmidt has to be mentioned here. This diatom builds up nuisance blooms in oligotrophic rivers (Spaulding and Elwell 2007, Kilroy and Bothwell 2012) and is outcompeted by other taxa such as *Spirogyra* spp. at increased P levels (Kilroy and Bothwell 2012). Similar to *Oocardium*, *Didymosphenia* is attached to the substratum via

gelatinous stalks. In the uppermost part of the stalks, high phosphatase activity was detected especially in rivers with increased organic P load, but low SRP availability (Ellwood and Whitton 2007). Extracellular phosphatase activity may also play an important role for *Oocardium* occurrence, but this hypothesis needs further studies.

Our reference site—Mayrbach rivulet—showed HCO_3^- and Ca_2^+ amounts comparable to those of the *Oocardium* rivulet, but no active carbonate precipitation. A possible explanation could be the increased SRP levels, as they strongly inhibit carbonate precipitation (Pentecost 2005). HCO_3^- levels of 4.7 mmol $\cdot$ L^{-1} and a temperature around 13.3°C provided optimal growth conditions for *O. stratum*. Both variables showed maxima during summer (Fig. 5) and reflect season as the background variable. At higher temperature, CO_2 solubility is further reduced, leading to increased CO_2 degassing during summer, which is an essential carbon source for *Oocardium* (Schagerl and Wukovits 2014).

The fast colonization of *O. stratum* in summer and associated calcium precipitation enabled the SAL layers to grow by up to 5 mm (Fig. 7); the gelatinous stalks of *Oocardium* provided perfect crystal nuclei. In the colder seasons, precipitation decreased due to a better CO_2 solubility; during this period, diatom mats prevailed. Both PCA factor scores (data not shown) and the RDA biplot revealed a clear pattern, which illustrated the seasonal alignment of chosen variables: increased *Oocardium* biomass, increased water temperatures and higher HCO_3^- levels coincided with the warmer period, while diatoms prevailed in the cold season and were mainly related to site openness and temperature (Figs. 5 and 6; Table S3), which is in accordance to previous studies. Diatoms as the dominant component are common in temperate rivers during the cold season followed by an increased contribution of green algae during summer (Kann 1978, Biggs 1996, Müllner and Schagerl 2003, Tekwani et al. 2013). In spring and autumn, just before leaves shoot and after leaves fall, microphytobenthos is often peaking because of increased irradiance conditions (Sumner and Fisher 1979, Müllner and Schagerl 2003). Total algae biomass in streams with constant discharge seems to be driven mainly by light supply, whereas water temperature controls the composition.

Mosses were not persistent. One explanation could be grazing by invertebrates or that moss propagules were overgrown by *O. stratum*. Compared to mosses, *O. stratum* seems to be more resistant against grazing due to its growth strategy with calcified mucilage tubes. A closer examination of the diatom community revealed taxa characteristic of SALs such as *Delicata delicatula* (Kützing) Krammer and *Encyonopsis microcephala* (Grunow) Krammer (Fig. 4; Cantonati et al. 2012c).

Why is *O. stratum* restricted to active SAL? The answer is probably linked to its specific carbon requirements and life strategy. Very recently, Schagerl and Wukovits (2014) found solely passive CO_2 uptake by *Oocardium*, which is available in excess in these habitats due to oversaturation. The first 15 m of the active precipitation showed no *Oocardium* colonies; the desmid colonized only the stretch downstream a certain distance from where precipitation started until the confluence with the Mayrbach Rivulet. This pattern was already recognized by Wallner (1934b) and Rott et al. (2010). *Oocardium* apparently occurs beginning at a specific distance from the spring over 2/3 of the full length of the active SAL depositions. At site A, flow velocity was reduced, while B to D showed more turbulence with increased water-air exchange. *Oocardium* clearly prefers sites with a high water-air exchange such as cascade splash-water zones. Here, CO_2 degassing is high and carbon uptake is probably most efficient. Carbonate deposition zones with laminar flow or pools under cascades did not show any *Oocardium* colonies, which points to the additional use of atmospheric CO_2 directly at the water/air interface. Compared to the diffusion coefficient of CO_2 in water (2.1×10^{-9} $m^2 \cdot s^{-1}$), CO_2 in air (1.4×10^{-5} $m^2 \cdot s^{-1}$) has a much higher diffusion coefficient (Martinez 2015) thus facilitating CO_2-uptake in these zones.

The growth strategy of *O. stratum* by its gelatinous stalk system is perfectly adapted to active SAL and protects colonies from grazing. The mucilage tubes themselves become calcified via abiotic calcification, which in our opinion is mainly passive. *Oocardium* colonies serve as a substratum, as do other surfaces. Rott et al. (2012) described four different types of *Oocardium* stalk calcification, among them granular initial calcification of the stalks by micritic crystallites below 1 μm consisting of low-magnesian calcite and initial precipitation of rhombohedral low-magnesia calcite. Those authors assumed that calcification types are driven by water chemistry, but this

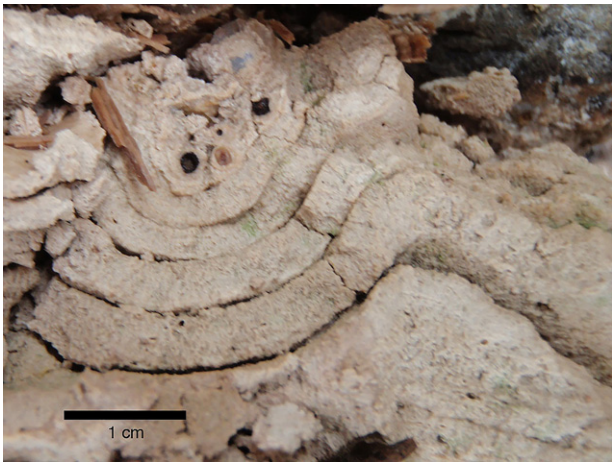

FIG. 7. Seasonal limestone lamination of primary travertine fabric at the *Oocardium* rivulet in the Mayrgraben, Lunz/See.

remains to be verified because extracellular polysaccharides and bacteria living therein might also be involved in this process.

Not only the stalk system of *Oocardium* is essential for attachment, but also for the exposure on the limestone surface to enable photosynthesis. Observations of increased colonization at sites with higher precipitation rates support this hypothesis. Nonetheless, it is still unclear whether higher growth rates induce elevated calcium precipitation or vice versa.

As already stated by Pfiester (1976), *Oocardium* might be more common in active SAL systems than expected, but these habitats are rarely visited by phycologists. Importantly, active and intact SAL combined with low nutrient concentrations are becoming fewer and fewer. As a result of deforestation, drainage pipes, well casing, artificial snow, micro-electric power generation and pollution, these peculiar habitats are disappearing (Cantonati et al. 2012a,b). Therefore, SAL (Sanders et al. 2011, Rott et al. 2012) have received protective status by the European Habitats Directive (EU HD 1992, Ellmauer and Traxler 2001). As *Oocardium* seems to be restricted to these SAL habitats, it is increasingly endangered.

This study was supported by a grant from the University of Vienna. We thank Hubert Kraill for ion analysis, the staff of the Wassercluster Lunz for technical support and Julia Wukowits for fruitful discussions. Marco Cantonati and Robert Krisai kindly verified identification of diatoms and mosses, respectively.

Apha. 2012. *Standard Methods for the Examination of Water and Wastewater*, 22nd edn. American Public Health Association, Washington, DC.

Battin, T. J., Kaplan, L. A., Newbold, J. D., Cheng, X. & Hansen, C. 2003. Effects of current velocity on the nascent architecture of stream microbial biofilms. *Appl. Environ. Microbiol.* 69:5443–52.

Besemer, K., Singer, G., Limberger, R., Chlup, A.-K., Hochedlinger, G., Hödl, I., Baranyi, C. & Battin, T. J. 2007. Biophysical controls on community succession in stream biofilms. *Appl. Environ. Microbiol.* 73:4966–74.

Biggs, B. J. F. 1996. Patterns in benthic algae of streams. *In* Stevenson, R. J., Bothwell, M. L. & Lowe, R. L. [Eds] *Algal Ecology – Freshwater Benthic Ecosystems*. Academic Press, Inc., San Diego, California, pp. 753.

Blenkinsopp, S. A. & Lock, M. A. 1994. The impact of storm-flow on river biofilm architecture. *J. Phycol.* 30:807–18.

Bothwell, M. L. 1989. Phosphorus-limited growth dynamics of lotic periphytic diatom communities: areal biomass and cellular growth rate responses. *Can. J. Fish Aquat. Sci.* 46:1293–301.

Brehm, V. & Ruttner, F. 1926. Die Biocönosen der Lunzer Gewässer. *Int. Rev. ges. Hydrobiol. Hydrogr.* 16:281–391.

Cantonati, M., Angeli, N., Bertuzzi, E., Spitale, D. & Lange-Bertalot, H. 2012c. Diatoms in springs of the Alps: spring types, environmental determinants, and substratum. *Freshw. Sci.* 31:499–524.

Cantonati, M., Füreder, L., Gerecke, R., Jüttner, I. & Cox, E. J. 2012a. Crenic habitats, hotspots for freshwater biodiversity conservation: toward an understanding of their ecology. *Freshw. Sci.* 31:463–80.

Cantonati, M., Rott, E., Spitale, D., Angeli, N. & Komárek, J. 2012b. Are benthic algae related to spring types? *Freshw. Sci.* 31:481–98.

Coesel, P. 2002. Find of *Oocardium* in Belgium. Available at http://www.desmids.nl/news/english/news_november_december_2002.html (accessed 5.6.2015).

Dormann, C. F. & Kühn, I. 2009. *Angewandte Statistik für die biologischen Wissenschaften*. Helmholtz Zentrum für Umweltforschung-UFZ, Halle, Germany, 257 pp.

Eberlein, K. & Kattner, G. 1987. Automatic method for the determination of ortho-phosphate and total dissolved phosphorus in the marine environment. *Fresenius Z. Für Anal. Chem.* 326:354–7.

Ellmauer, T. & Traxler, A. 2001. *Handbuch der FFH-Lebensraumtypen Österreichs*. Umweltbundesamt-Monographien, 130, 208 pp.

Ellwood, N. T. W. & Whitton, B. A. 2007. Importance of organic phosphate hydrolyzed in stalks of the lotic diatom *Didymosphenia geminata* and the possible impact of atmospheric and climatic changes. *Hydrobiologia* 592:121–33.

EU HD (European Union habitat directive). 1992. European Commission, Environment Directorate-General: Council Directive 92/43/EEC of 21 May 1992 on the conservation of natural habitats and of wild fauna and flora. *Off. J. Eur. Union L.* 206:7–50.

Faupl, P. 2003. *Historische Geologie: Eine Einführung*, 2nd edn. UTB, Stuttgart, 271 pp.

Frazer, G. W., Canham, C. D. & Lertzman, K. P. 1999. *Gap Light Analyzer (GLA), Version 2.0: Imaging Software to Extract Canopy Structure and Gap Light Transmission Indices from True-colour Fisheye Photographs, Users Manual and Program Documentation*. Simon Fraser University/Institute of Ecosystem Studies, Burnaby, British Columbia/Millbrook, New York and Burnaby, British Columbia.

Golubić, S. & Marčenko, E. 1958. Zur Morphologie und Taxonomie der Desmidiaceengattung *Oocardium*. *Schweiz. Z. Für Hydrol.* 20:177–85.

Götzinger, G. 1910. Die Lunzer Seen, I. Teil: Physik. A. Geomorphologie der Lunzer Seen und ihres Gebietes. *Arch. Hydrobiol. Suppl.* 3:1–154.

Hainz, R., Wöber, C. & Schagerl, M. 2009. The relationship between *Spirogyra* (Zygnematophyceae, Streptophyta) filament type groups and environmental conditions in Central Europe. *Aquat. Bot.* 91:173–80.

Hansgirg, A. 1905. Grundzüge der Algenflora von Niederösterreich. *Beih. Bot. Cent.bl.* 18:417–522.

Hofmann, G., Werum, M. & Lange-Bertalot, H. 2011. *Diatomeen im Süßwasser-Benthos von Mitteleuropa*. Gantner, Rugell, 908 pp.

Kann, E. 1978. Systematik und Ökologie der Algen österreichischer Bergbäche. *Arch. Hydrobiol. Suppl.* 53:405–643.

Kempers, A. J. & Luft, A. G. 1988. Re-examination of the determination of environmental nitrate as nitrite by reduction with hydrazine. *Analyst* 113:1117–20.

Kilroy, C. & Bothwell, M. L. 2012. *Didymosphenia geminata* growth rates and bloom formation in relation to ambient dissolved phosphorus concentration. *Freshw. Biol.* 57:641–53.

Krammer, K. & Lange-Bertalot, H. 2004-2008. *Süßwasserflora von Mitteleuropa*, Bacillariaceae. Naviculaceae, 2/1, 876 pp.; Bacilariaceae, Epithemiaceae, Surirellaceae, 2/2, 610 pp.; Centrales, Fragilariaceae, Eunotiaceae, 2/3, 598 pp.; Achnantaceae, 2/4, 468 pp. Fischer, Stuttgart and New York.

Legler, C. 1988. *Ausgewählte Methoden der Wasseruntersuchung: Chemische, physikalisch-chemische und physikalische Methoden*. Gustav Fischer Verlag, Jena, 517 pp.

Leichtfried, M. 1990. Organische Substanz in Bettsedimenten des Oberen Seebaches in Lunz/See. *Niederösterreich. Mitt. Österr. Geol. Ges.* 83:229–41.

Lenzenweger, R. 2003. *Desmidiaceenflora von Österreich, Teil 4*. Bibliotheca Phycologica 111, J. Cramer, Stuttgart, 87 pp.

Leyer, I. & Wesche, K. 2008. *Multivariate Statistik in der Ökologie: Eine Einführung*. 1. Aufl. 2007, Korr. Nachdruck 2008 edition, Springer, Berlin, Heidelberg, 221 pp.

Martinez, I. 2015. Available at http://webserver.dmt.upm.es/~isidoro/dat1/Mass%20diffusivity%20data.pdf (accessed 5.6.2015).

Mathews, H. L., Prescott, G. W. & Obenshain, S. S. 1965. The genesis of certain calcareous floodplain soils of Virginia. *Soil Sci. Soc. Am. J.* 29:729–32.

Moreno Alcaraz, J. L., Monteagudo Canales, L. & Aboal Sanjurjo, M. 2013. Morphological description and ecology of some rare macroalgae in south-central Spanish rivers (Castilla-La Mancha Region). *An. Jardín Botánico Madr.* 70:81–90.

Müllner, A. & Schagerl, M. 2003. Abundance and distribution of the phytobenthic community in an alpine gravel brook. *Internat. Rev. Hydrobiol.* 88:243–54.

Nägeli, C. 1849. Gattungen einzelliger Algen, physiologisch und systematisch bearbeitet. *Neue Denkschr. Allg. Schweiz. Ges. Naturw.* 10:1–139.

Oksanen, J. 2011. *Multivariate analysis of ecological communities in R: vegan tutorial.* 1. Univ. Oulu, Finland. http://cc.oulu.fi/jarioksa/opetus/metodi/vegantutor.pdf

Oksanen, J., Kindt, R., Legendre, P., O'Hara, B., Simpson, G. L., Solymos, M., Stevens, M. H. H. & Wagner, H. 2007. *The Vegan Package. Community Ecology Package.* Version 1.15-1.

Passy, S. I. & Larson, C. A. 2011. Succession in stream biofilms is an environmentally driven gradient of stress tolerance. *Microb. Ecol.* 62:414–24.

Pentecost, A. 1981. The tufa deposits of the Malham district. *Field Stud.* 5:365–87.

Pentecost, A. 1991. A new and interesting site for the calcite-encrusted desmid *Oocardium stratum* Naeg. in the British Isles. *Br. Phycol. J.* 26:297–301.

Pentecost, A. 1993. British travertines: a review. *Proc. Geol. Ass.* 104:23–39.

Pentecost, A. 2005. *Travertine.* Springer, Berlin, Heidelberg, 446 pp.

Pentecost, A. & Zhang, Z. 2000. The travertine flora of Juizhaigou and Munigou, China, and its relationship with calcium carbonate deposition. *Cave Karst Sci.* 27:71–8.

Pfiester, L. A. 1976. *Oocardium stratum* a rare (?) desmid (Chlorophyceae). *J. Phycol.* 12:134.

R Core Team. 2014. *R: A Language and Environment for Statistical Computing.* R Foundation for Statistical Computing, Vienna, Austria. Available at http://www.R-project.org/ (accessed 5.6.2015).

Ramette, A. 2007. Multivariate analyses in microbial ecology. *FEMS Microbiol. Ecol.* 62:142–60.

Rasband, W. S. 1997-2014. *ImageJ.* U.S. National Institutes of Health, Bethesda, Maryland. Available at http://imagej.nih.gov/ij/ (accessed 5.6.2015).

Rieth, A. 1969. Suesswasserarten-Algenarten in Einzeldarstellung II. *Oocardium stratum* nach Material aus Kuba. *Kult.* XVIII:51–71.

Rott, E., Holzinger, A., Gesierich, D., Kofler, W. & Sanders, D. 2010. Cell morphology, ultrastructure, and calcification pattern of *Oocardium stratum*, a peculiar lotic desmid. *Protoplasma* 243:39–50.

Rott, E., Hotzy, R., Cantonati, M. & Sanders, D. 2012. Calcification types of *Oocardium stratum* Nägeli and microhabitat conditions in springs of the Alps. *Freshw. Sci.* 31:610–24.

Sanders, D. & Rott, E. 2009. Contrasting styles of calcification by the micro-alga *Oocardium stratum* Naegeli 1849 (Zygnematophyceae) in two limestone-precipitating spring creeks of the Alps *Oocardium stratum. Austrian J. Earth Sci.* 102:34–49.

Sanders, D., Wertl, W. & Rott, E. 2011. Spring-associated limestones of the Eastern Alps: overview of facies, deposystems, minerals, and biota. *Facies* 57:395–416.

Schagerl, M. & Pröschold, T. 2007. Rediscovery of *Oocardium stratum* Näg. *in* Smolenice-Castle, V. [Ed] *Austria and its preliminary taxonomic position within the Desmidiales.* Proceedings of Biology and Taxonomy of Green Algae.

Schagerl, M. & Wukovits, J. 2014. Cultivation and inorganic carbon uptake of the rare desmid *Oocardium stratum* (Conjugatophyceae). *Phycologia* 53:320–8.

Sumner, W. T. & Fisher, S. G. 1979. Periphyton production in Fort River, Massachusetts. *Freshw. Biol.* 9:205–12.

Spaulding, A. S. & Elwell, L. 2007. Increase in nuisance blooms and geographic expansion of the freshwater diatom *Didymosphenia geminata.* Open-File Report 2007–1425. Available at https://www.fort.usgs.gov/sites/default/files/products/publications/22046/22046.pdf (accessed 15 August 2015).

Tekwani, N., Majdi, N., Mialet, B., Tornés, E., Urrea-Clos, G., Buffan-Dubau, E., Sabater, S. & Tackx, M. 2013. Contribution of epilithic diatoms to benthic-pelagic coupling in a temperate river. *Aquat. Microb. Ecol.* 69:47–57.

Tollmann, A. 1965. *Geologie der Kalkvoralpen im Ötscherland als Beispiel alpiner Deckentektonik.* Mitteilungen der Geologischen Gesellschaft in Wien, 58, Band, pp. 103–207.

Wallner, J. 1933. Zur Kenntnis der Gattung *Oocardium. Hedwigia.* 75:130–6.

Wallner, J. 1934a. *Oocardium stratum* Näg., eine wichtige tuffbildende Alge Südbayerns. *Planta* 20:287–93.

Wallner, J. 1934b. Über die Verbreitungsökologie der Desmidiaceae *Oocardium. Planta* 23:249–63.

Wallner, J. 1934c. Über die Beteiligung kalkablagernder Pflanzen bei der Bildung südbayerischer Tuffe. *Bibliotheca botanica* 110:1–30.

Whitton, B. A., Al-Shehri, A. H., Ellwood, N. T. W. & Turner, B. L. 2005. Ecological aspects of phosphatase activity in cyanobacteria, eukaryotic algae and bryophytes. *In* Turner, B. L., Frossard, E. & Baldwin, D. S. [Eds] *Organic Phosphorus in the Environment.* Commonwealth Agricultural Bureau, Wallingford, UK, pp. 205–41.

Whitton, B. A. & Neal, C. 2011. Organic phosphate in UK rivers and its relevance to algal and bryophyte surveys. *Ann. Limnol. Int. J. Lim.* 47:3–10.

ZAMG. 2000-2013. Available at https://www.zamg.ac.at/cms/de/klima/klimauebersichten/jahrbuch (accessed 5.6.2015).

Supporting Information

Additional Supporting Information may be found in the online version of this article at the publisher's web site:

Figure S1. Seasonal algal cover comparison of sites B to D from 16.4.2008 until 24.7.2009.

Table S1. Loadings of transformed environmental variables of the three factors extracted by factor analysis. (loadings >0.5 are marked with an asterisk for better visibility). Abbreviations: lightsum (radiation week sum), cond (conductivity), Q (discharge), temp.abs (temperature in °K).

Table S2. Summary statistics and results of ANOVA for the whole model and for the first axis of redundancy analysis of all *Oocardium* sites.

Table S3. Weighted averages of all factors for algal taxa (values >0.3 marked by an asterisk for better visibility). Abbreviations: temp.abs (temperature, °K), lightsum (weekly sum of radiation, klx), SiteO (Site Openness, %).